Published in Geologica Acta 8, issue 1, 67-82, 2010
which should be used for any reference to this work

Conductive structures around Las Cañadas caldera, Tenerife (Canary Islands, Spain): A structural control

N. COPPO P.A. SCHNEGG |*| P. FALCO and R. COSTA

Geomagnetism group, Department of Geology, University of Neuchâtel
CP 158, 2009 Neuchâtel, Switzerland

*corresponding author E-mail: pierre.schnegg@unine.ch

ABSTRACT

External eastern areas of the Las Cañadas caldera (LCC) of Tenerife (Canary Islands, Spain) have been investigated using the audiomagnetotelluric (AMT) method with the aim to characterize the physical rock properties at shallow depth and the thickness of a first resistive layer. Using the results of 50 AMT tensors carried out in the period range of 0.001 s to 0.3 s, this study provides six unpublished AMT profiles distributed in the upper Orotava valley and data from the Pedro Gil caldera (Dorsal Ridge). Showing obvious 1-D behaviour, soundings have been processed through 1-D modeling and gathered to form profiles. Underlying a resistive cover (150-2000 Ωm), a conductive layer at shallow depth (18-140 Ωm, 250-1100 m b.g.l.) which is characterized by a "wavy-like" structure, often parallel to the topography, appears in all profiles. This paper points out the ubiquitous existence in Tenerife of such a conductive layer, which is the consequence of two different processes: a) according to geological data, the enhanced conductivity of the flanks is interpreted as a plastic breccia within a clayish matrix generated during huge lateral collapse; and b) along main tectonic structures and inside calderas, this layer is formed by hydrothermal alteration processes. In both areas, the conductive layer is thought to be related to major structural volcanic events (flank or caldera collapse) and can be seen as a temporal marker of the island evolution. Moreover, its slope suggests possible headwall locations of the giant landslides that affected the flanks of Tenerife.

KEYWORDS **Magnetotelluric method. Caldera. Hydrothermal alteration. Lateral collapse. Tenerife.**

INTRODUCTION

The knowledge of volcanic structures is an essential prerequisite to understanding eruption types and dynamics (Aizawa et al., 2005). Resistivity surveys are one way to highlight this invisible part of a volcano. Often being free of EM cultural noise, many volcanic areas are investigated with EM methods and most of these studies reveal conductive layers. For example, in the Reunion Island, these layers are interpreted as poorly permeable clayey material that controls the groundwater (Courteaud et al., 1997; Descloitres et al., 1997; Boubekraoui et al., 1998) or as horizons belonging to ancient phases of the volcanoes (Schnegg, 1997). At Merapi volcano (Müller and Haak, 2004), at Kusatsu-Shirane volcano (Nurhasan et al., 2006) and in Terceira Island (Monteiro Santos et al.,

2006) shallow conductive zones were interpreted as due to geothermal fluids. At Mt Fuji volcano, a central conductive body is interpreted as an active hydrothermal system (Aizawa et al., 2005), just as it is for the Somma-Vesusius volcano (Manzella et al., 2004). At Usu volcano (Ogawa et al., 1998), conductive bodies are related to altered rocks and a major dyke. On Izu-Oshima Island, Ogawa and Takakura (1990), using data from nearby wells, interpreted their deep conductive layer as thermal water. In the Las Cañadas caldera (LCC), conductive bodies have been interpreted as altered rocks or groundwater bodies (Pous et al., 2002). These examples highlight the wide range of existing conductive layers or bodies in volcanic areas, and often the difficulty interpreting their nature in absence of constraining geological or borehole data.

In Tenerife, two previous magnetotelluric (MT) works (Ortiz et al., 1986; Pous et al., 2002) investigated the Las Cañadas caldera and the Teide - Pico Viejo Complex (TPVC, Fig. 1) in an attempt to reveal both the deep and shallow structures of the central part of Tenerife. Recently, we carried out a detailed AMT survey of the LCC (Coppo et al., 2007b) and the Icod valley (Coppo et al., 2007a) to map the top conductive layer previously discovered by Pous et al. (2002). Our results led us to carry on geophysical investigations outside the LCC where fifty

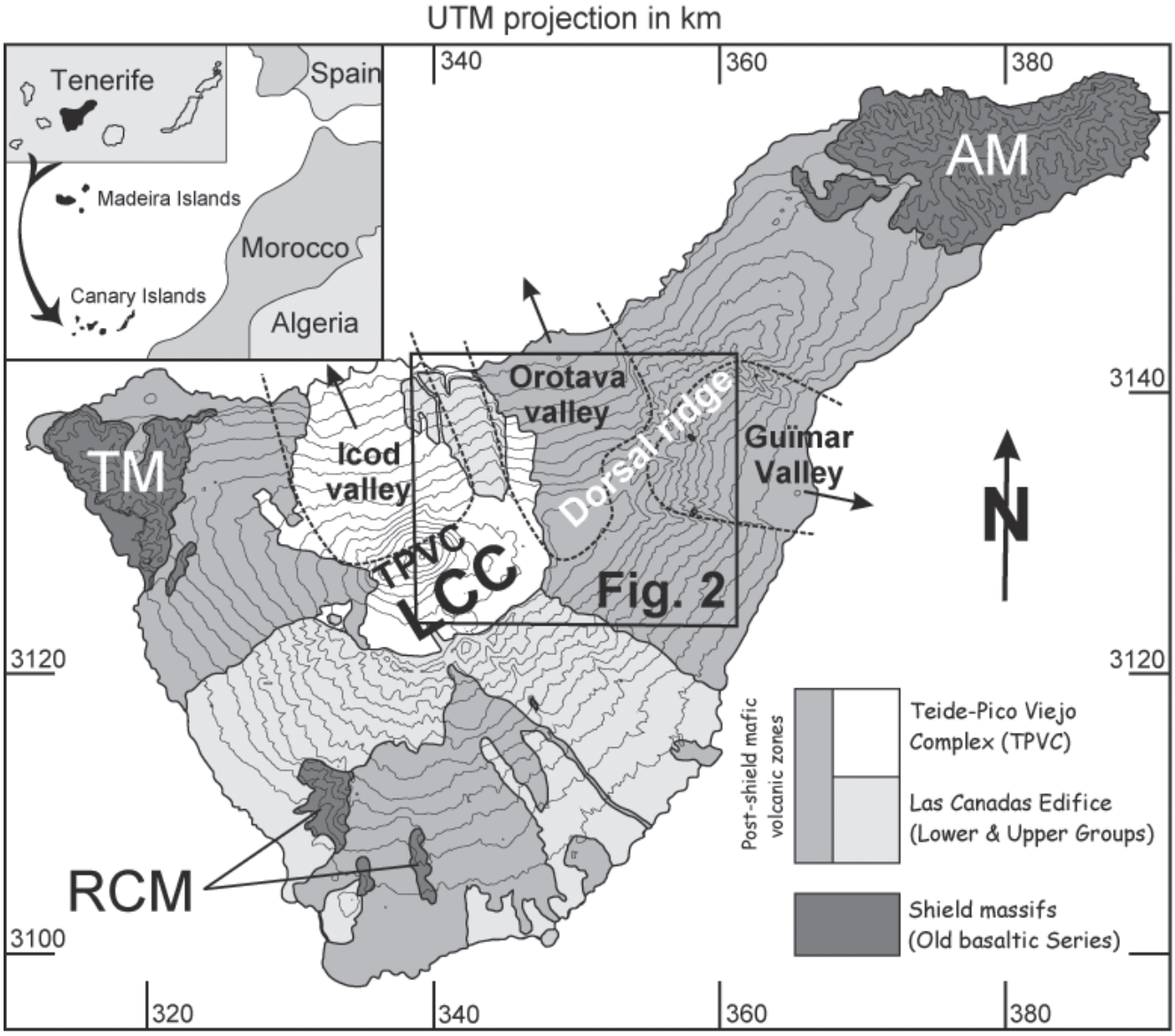

FIGURE 1 | **Geological sketch of Tenerife. Inset: Location of Tenerife. Black rectangle: Map of figure 2. The dashed lines show the trace of three valleys initiated by lateral collapse. TM= Teno Massif; AM= Anaga Massif; RCM= Roque del Conde Massif; LCC= Las Cañadas caldera. TPVC= Teide - Pico Viejo Complex.**

new AMT soundings have been measured in four different areas (respectively Orotava valley, Fasnia - Siete Fuentes, Guïmar valley and Pedro Gil caldera, Fig. 2). This study aims at determining: i) the thickness and resistivity of the first layer; ii) the resistivity of the second, generally conductive, layer and comparing the results obtained in different geological provinces of the central part of Tenerife. With similar objectives, the Pedro Gil caldera has also been investigated (Fig. 2). There, a recent detailed structural study of this caldera proposes geological cross-sections and interpretations that geophysics may help to constrain.

THE AUDIOMAGNETOTELLURIC METHOD

The MT method is a passive surface geophysical technique that uses the earth's natural EM fields to investigate the electrical resistivity structure of the subsurface from depth of tens of meters to tens of km (Vozoff, 1991). The AMT is a part of MT that uses high frequency, above 1 Hz, generated by the worldwide thunderstorm activity. EM signals penetrate into the earth at various depths depending on the earth's conductivity and the signal frequency. Assuming that EM energy penetrates vertically into the earth as a plane wave, one can determine the variation

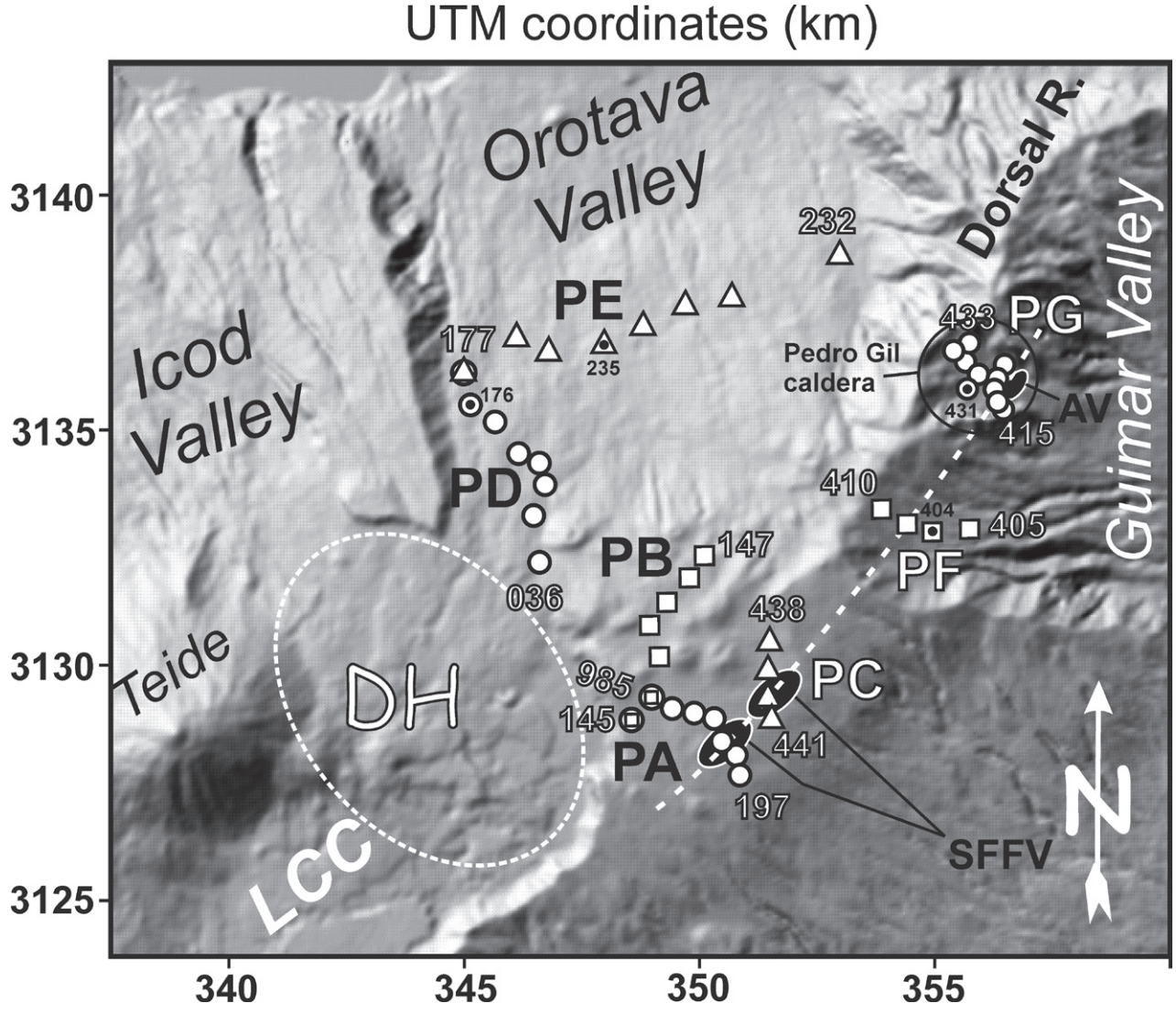

FIGURE 2 | **Shaded relief map of the prospected area. Location of 6 profiles (PA to PF) and the Pedro Gil caldera (PG). White symbols indicate AMT soundings belonging to different profiles. Names of soundings are indicated for the first and last site of each profile. AMT sites with a black dot and name show typical 1D sites presented on Fig. 3. The three valleys resulting from lateral landslides are indicated in italics. Diego Hernandez (DH) caldera is circumscribed by a white dashed ellipse. The eastern dashed white line corresponds to the fracture thought to be responsible for the Fasnia, Siete Fuentes and Arafo eruptions (Valentin et al., 1990). The four black elliptic zones located on PA, PC and PG profiles correspond to historical eruptions: Siete Fuentes (1704), Fasnia (1705) (SFFV) and Arafo (1705) volcano (AV), respectively.**

of resistivity with depth by surface measurements of the electric and magnetic fields as a function of frequency. The depth of penetration of EM waves is controlled by the skin effect. The MT theory may be found in the basic paper of Cagniard (1953) and further details in Simpson and Bahr (2005). MT and AMT methods are currently used in many domains of applied and research geophysics such as mineral exploration, geothermal reservoir and internal structures of volcanoes (e.g., Benderitter and Gérard (1984), Ballestracci and Nishida (1987), Courteaud et al. (1997), Schnegg (1997), Ogawa et al. (1998), Fuji-ta et al. (1999), Matsushima et al. (2001), Manzella et al. (2004), Nurhasan et al. (2006)).

We used an AMT recording system developed at the University of Neuchâtel, light enough to be carried by two walking persons. The four horizontal components of the field were measured in the N-S and E-W directions in the period range from 0.001 to 0.3 s at a sampling rate of 2 kHz. Fifty meter-long telluric lines were arranged orthogonally and connected to non-polarizable electrodes made of acrylic tubes ended with a porous ceramic. Inside the tube, a non-polarizable Ag-AgCl electrode designed for ocean studies (Filloux, 1987) was immersed in a saturated KCl solution. Magnetic induction coils (two ECA CM16) were set up orthogonally in the middle of the station.

GEOLOGICAL SETTING

General

Tenerife, the largest island of the Canarian archipelago, lies a few hundred kilometers off the African coast (Fig. 1). It is home to the second largest oceanic island volcanic complex in the world after Mauna Loa and Mauna Kea in Hawaii. The sub aerial portion of the island known as the Old Basaltic Series (Fúster et al., 1968) is a composite mafic alkaline formation constructed by fissure eruptions of ankaramites, basanites and alkali basalts between 12 and 3.5 Ma (Abdel-Monem et al., 1972; Ancochea et al., 1990) and now preserved at the three corners of the island: the Anaga peninsula (NE), the Teno massif (NW) and the Roque del Conde (S) (Fig. 1). Toward the end of this period, volcanic activity concentrated in the central part of Tenerife, where shallow phonolitic magma chambers developed to form a central volcanic complex, the Las Cañadas edifice (LCE). Of basaltic to phonolitic composition, it was constructed and modified by several volcanic cycles (Araña, 1971; Ancochea et al., 1990; Marti et al., 1994; Ancochea et al., 1999).

Following Marti et al. (1994), the LCE includes both a complex and poorly studied Lower Group (3.5-2 Ma), and an Upper Group (1.6-0.17 Ma). The Lower group includes up to 7 units mainly outcropping in the lower part of the caldera wall, and is composed of phonolitic, basaltic lava and minor pyroclastic rocks, including phonolitic welded tuff (Marti et al., 1994). The Upper Group consists of three formations: Ucanca (1.54-1.07 Ma), Guajara (0.85-0.57 Ma) and Diego Hernandez (0.38-0.18 Ma), each of which ended by caldera collapse (Marti et al., 1994; Marti et al., 1997; Coppo et al., 2007b). This overlapping collapse process is attributed to the eastward migration of a shallow magma chamber (Marti and Gudmundsson, 2000).

The Orotava valley

The Orotava valley (Figs. 1 & 2) is a large and deep scar affecting the northern flank of Tenerife. It results from a lateral landslide (Teide Group, 1997) and is infilled by a significant amount of post-slide volcanic deposits from the volcanic centers along the Dorsal rift zone (Figs. 1 & 2) and by mafic to intermediate lava flows from eruptive vents inside the LCC. A simplified geology of the area shows two main rock sequences: the pre-slide (> 0.56 Ma) and the post-slide deposits (< 0.56 Ma) (Hürlimann et al., 2004; Galindo, 2005). At the western border of the valley, the Tigaiga massif is composed of intermediate to phonolitic lavas and phonolitic pyroclastics belonging to Las Cañadas edifice. It represents a remnant between the Orotava and the Icod valleys, unaffected by the landslide events (Ibarrola et al., 1993; Marti, 1998). At the eastern part of the amphitheatre, the pre-slide deposits are characterized by mafic lava flows from eruptive vents located along the Dorsal ridge (Fig. 2). Post-slide deposits almost cover the entire valley floor, with thickness in excess of 500 m in some locations (Servicio de Planificatión Hydráulica, 1991). These deposits consist mainly of valley-filling breccia. They were identified in the water tunnel drilled in the Orotava valley (Coello, 1973). Chronostratigraphic data suggest that the formation of the valley coincided with the episode of vertical collapse, interpreted as the end of the Guajara cycle (Marti et al., 1997).

The Fasnia - Siete Fuentes area

Disregarding the central system eruptions (TPVC), eight historic eruptions occurred in Tenerife. Two of them, the Siete Fuentes (1704 ad.) and Fasnia (1705 ad.) basaltic fissural eruptions occurred outside the eastern part of the LCC (Fig. 2). These igneous centres are aligned on the NE-SW major fracture, parallel to one of the predominant tectonic lines of the island (Valentin et al., 1990). The fracture can be followed to the Pedro Gil caldera (Fig. 2) in which the historical eruption of the Arafo volcano occurred simultaneously (1705 ad.). Abnormal temperatures (up to 45°C), high concentration of heat flow indicators (SiO_2, B, NH_4^+), gases (CO_2, H_2, CH_4) and very high content of CO_3H^+ and SO_4^{+2} related to the recent volcanism are found

to the south of the Siete Fuentes and southeast of Fasnia volcanoes (Valentin et al., 1990; Navarro Latorre, 1996).

Although geothermal activity is not manifest in these areas, Rn anomalies prove the existence of upwelling geothermal fluids through several fractures located beneath the Fasnia and Siete Fuentes volcanoes, indicating higher temperatures at depth (Hernández et al., 2003). Geothermometry techniques applied to the central system of Teide have shown that the temperature of the residual magma body of Fasnia - Siete Fuentes was 270 ± 50°C (Valentin et al., 1990).

The Guïmar valley

The Guïmar valley is located on the SE part of Tenerife (Figs. 1 & 2). From on- and off-shore surveys (Krastel et al., 2001; Masson et al., 2002), it was interpreted as the result of a catastrophic flank failure. The sub aerial Guïmar valley is approximately 10 km wide with a relatively well-defined flat base and flanking scarps from 300 up to 600 m high. In its upper part, the Guïmar valley forms two diverging sub-valleys separated by a low ridge. Both sub-valleys extend onto the narrow Dorsal ridge that separates the Orotava and Guïmar valleys (Masson et al., 2002). The Guïmar valley has no obvious relationships with any caldera-forming episode. However, based on its morphology and presence of deposits of Guajara age, it is older than the Orotava valley (Marti et al., 1997). No mention was found regarding the thickness of the deposits or the presence of breccia at its base.

The Pedro Gil caldera

The Pedro Gil caldera is roughly located on the NE Dorsal Ridge of Tenerife (Fig. 2). Its size is approximately 3 km in diameter and 540 m deep. However, assuming vertical collapse, its true diameter could be only 1.5 km and its depth 700 m (Galindo, 2005). A paleomorphologic analysis suggests that it formed about 0.81 Ma ago (Ancochea et al., 1990) by the vertical collapse of the Pedro Gil edifice (Galindo, 2005). The development of this edifice is summarized by Galindo (2005) as follows: a) a magma intrusion causes up doming of the surface; b) the magmatic overpressure leads the magma injection through tilted sheets and radial dykes causing effusive eruption; c) the subsidence of the magmatic column leaves a cavity at the top of the column; and d) the roof of the cavity collapses, creating the caldera. Geologically, the Pedro Gil formation makes the caldera walls. Lava flows of unknown thickness and pyroclastic deposits of historical eruptions filled in the bottom of the caldera (Galindo, 2005). Recently, this author suggested that the formation of the Guïmar valley could be associated with the Pedro Gil volcano collapse and the formation of its caldera. A historical eruption created the Arafo volcano in 1705 (Fig. 2), a consequence of the SW-NE fissural activity related to the Fasnia – Siete Fuentes volcanoes.

RESULTS

Dimensionality and data processing

The results presented in this paper include all soundings acquired outside the LCC during three field campaigns carried out in 2004, 2005 and 2006. The locations of the 50 AMT sites collected in the eastern sector of the LCC are shown in Fig. 2. Except for a few soundings affected by cultural EM disturbances, the overall data quality is very good. Most of the data show a uniform, close to 1-D behaviour and display similar results in the whole area, in good agreement with Pous et al. (2002). The shape of the apparent resistivity and phase curves reveals a resistive layer overlying a conductive layer (Fig. 3). Although, at times, a third layer appears at depth, enabling an estimation of the thickness of the conductive layer, we only focus on the thickness of the first layer and the resistivity of the two first layers. Only a few soundings display curve splitting at higher and lower frequencies due to shallow heterogeneities or signal weakness (Fig. 3, 4th site). Invariants of the determinant of all impedance tensors have been modelled separately (Fig. 3) using a 1-D modelling scheme (Fischer and Le Quang, 1981; Schnegg, 1993). Then, subtracting the thickness of the first resistive layer from the altitude, new elevations were interpolated to visualise the morphology of the top of the conductive layer along profiles or over the Pedro Gil caldera area. Coast effect that affects low frequencies was ignored since its influence starts at 5 s. (Pous et al., 2002; Monteiro Santos et al., 2006).

Static shift

The magnetotelluric (MT) static shift is a galvanic distortion effect that locally affects apparent resistivity sounding curves, shifted by a frequency-independent factor, keeping the phases unchanged (Simpson and Bahr, 2005). The rotation of the impedance tensors reveals that static shift does not significantly affect our data. Figure 4 presents two AMT tensors (192 and 193) from profile PA (Fig. 5). Both are rotated first in the direction of the profile ($\theta = 126°$, then by $\theta + 45°$) and illustrate the presence of a negligible static shift effect. In addition, detailed pseudosections of apparent resistivity (ρ_{xy} and ρ_{yx}) and phase (φ_{yx} and φ_{yx}) of the profile PA are shown in figure 5. The upper part of figure 5 A) presents the profile PA where the AMT site 194 has been removed. It is characterized by an obvious 1-D behaviour. Below that (Fig. 5, B), site 194 has been kept. The ρ_{xy} pseudosection remained absolutely unchanged but the ρ_{yx} and φ_{yx} pseudosections show a 2-D effect. Figure

5 is representative of the 1-D character of the AMT sites measured in the central part of Tenerife, with very few 2-D effects. Thus, the straightforward 1-D approach was applied using the invariant of the impedance tensors.

AMT profiles

The Fasnia - Siete Fuentes area has been investigated through 17 AMT soundings gathered in three profiles (PA, PB and PC, Fig. 2). Two of them (PA - Fig. 5 and PC - Fig. 6) cross the SW-NE fissure (Fig. 2). The first profile (PA, Fig. 5) crosses the Fasnia fissural eruption of 1703. High resistivity ranges from 700 to 1800 Ωm and low resistivity from 35 to 100 Ωm. The thickness of the resistive layer ranges from 500 to 800 m. The top of the conductor presents a wavy morphology at 0.8 and 2.3 km. The second profile (PB, Fig. 6) extends along 3.4 km and also reveals a wavy morphology of the top conductive layer with a wavelength

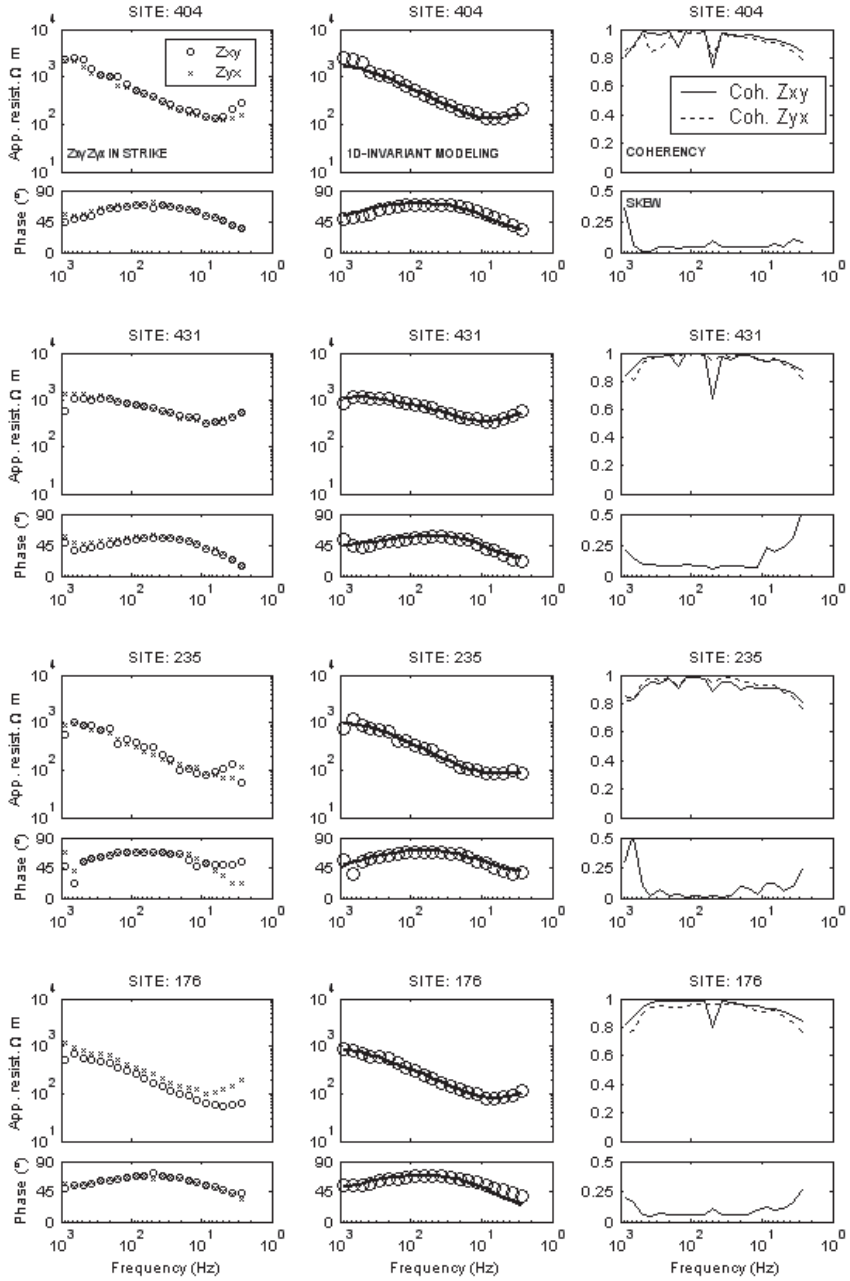

FIGURE 3 | **Typical 1D AMT soundings. 1st column) Apparent resistivity, phase for both Zxy and Zyx tensor elements vs. period in direction of the maximum phase anisotropy. 2nd column) 1D modelling of the invariant of the impedance tensor (Z = ZxxZyy – ZxyZyx). The black line is the model response). 3rd column) Coherency and skewness after Swift (1967).**

of almost 2 km. It is characterized by three highs separated by two depressions (1.3 and 3 km) of 400 m depth. High resistivities range from 700 to 2000 Ωm and low resistivity from 35 to 100 Ωm. The thickness of the resistive layer ranges from 500 to 800 m. The third profile (PC, Fig. 6) includes 4 AMT soundings. High resistivities range from 1200 to 1600 Ωm and low resistivity from 50 to 100 Ωm. The thickness of the resistive layer ranges from 500 to 800 m. This profile shows a conductive layer almost parallel to the surface with resistivity slightly increasing southwards.

Fifteen soundings have been recorded in the Orotava valley (Fig. 2) and gathered in two profiles (PD and PE, Fig. 6). Profile PD is parallel and PE is transverse to the valley. Results of both profiles show a ~500 m-thick resistive layer (400-1000 Ωm) overlaying a conductive one (< 50 Ωm).

Because of the steep, hardly accessible morphology characterizing the top of the Guïmar valley, only four soundings could be measured over the 1.75 km-long profile (profile PF, Fig. 2). One-D models were assembled to build the resistivity profile PF (Fig. 7). High resistivities range from 700 to 1600 Ωm and low resistivity from 35 to 70 Ωm. The thickness of the resistive layer ranges from 530 to 980 m. The main morphology highlighted is the steep ascent of the top conductive layer between sites 410 and 401 showing 32% uphill and 68% downhill dips and 31% between sites 401 and 405.

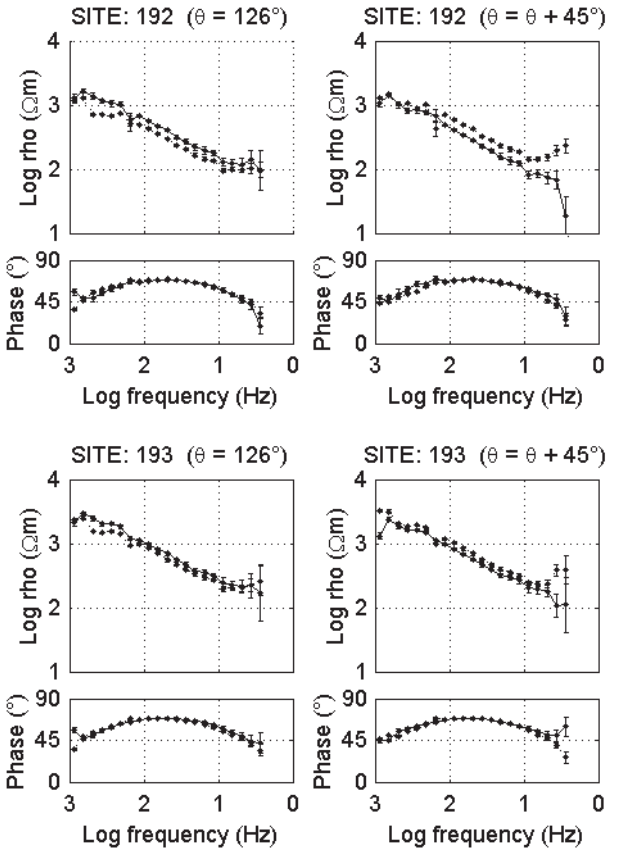

FIGURE 4 | **Two AMT sites (192 and 193) of profile PA (Fig. 2) with matrices rotated 1. (left) in the direction of the profile (θ = 126) and 2. (right) to an angle of θ + 45°. The small variation of ρ_{app} indicates a negligible static shift effect**

Given the poor accessibility, ten soundings were measured in the small Pedro Gil caldera (Figs. 2 & 8). As for the Guïmar valley, this area is absolutely free of cultural EM disturbances, resulting in high data quality. Because of the scattered distribution of soundings, results of the 1-D models have been converted into interpolated maps (Fig. 8). High resistivities range from 140 to 970 Ωm (Fig. 8A) and low resistivities from 35 to 245 Ωm (Fig. 8B). The thickness of the resistive layer ranges from 270 to 970 m (Fig. 8C). Higher resistivities of both the resistor and the conductor are observed in the central part of the caldera. Likewise, the maximum thickness (soundings 417, 419 and 431) is obtained in the same area characterized by a depression of the top conductive layer. While the conductive layer is well marked on the eastern part of the Pedro Gil caldera, its quasi absence should be noted in the western part. Although all sites were almost 1-D, we looked for the maximum phase anisotropy by rotating the MT impedance tensors. Figure 8A shows strike direction (modulo 180°) for the ten AMT soundings carried out in the Pedro Gil caldera.

INTERPRETATIONS - DISCUSSION

All the profiles presented in this study highlight the presence of a conductive layer at shallow depth. Together with the results of previous studies (Ortiz et al., 1986; Pous et al., 2002; Coppo et al., 2007a; Coppo et al., 2007b), these data suggest its ubiquitous existence, at least in the central part of Tenerife. Such a shallow conductive layer has been discovered in many volcanic environments and interpreted in many different ways (see references in introduction). In Tenerife, the conductive layer is characterized by a general resistivity below 100 Ωm. It is overlaid by a resistive cover (> 400 Ωm), generally 0.5 to 1 km thick. As shown in Figures 3, 4 and 5, the data present a near 1-D behavior with negligible static shift effect. Although very few AMT stations may be affected by 2-D effects (Fig. 5, site 194), the 1-D modeling approach has been chosen to track the shallow architecture of the eastern part of the Las Cañadas caldera.

The general morphology of the top conductive layer is approximately parallel to the surface, but displays undulations of various wavelengths (Figs. 5, 6 & 7). This "wavy-like" structure is interpreted as a consequence of the structural setting of the studied area. Our studies carried out

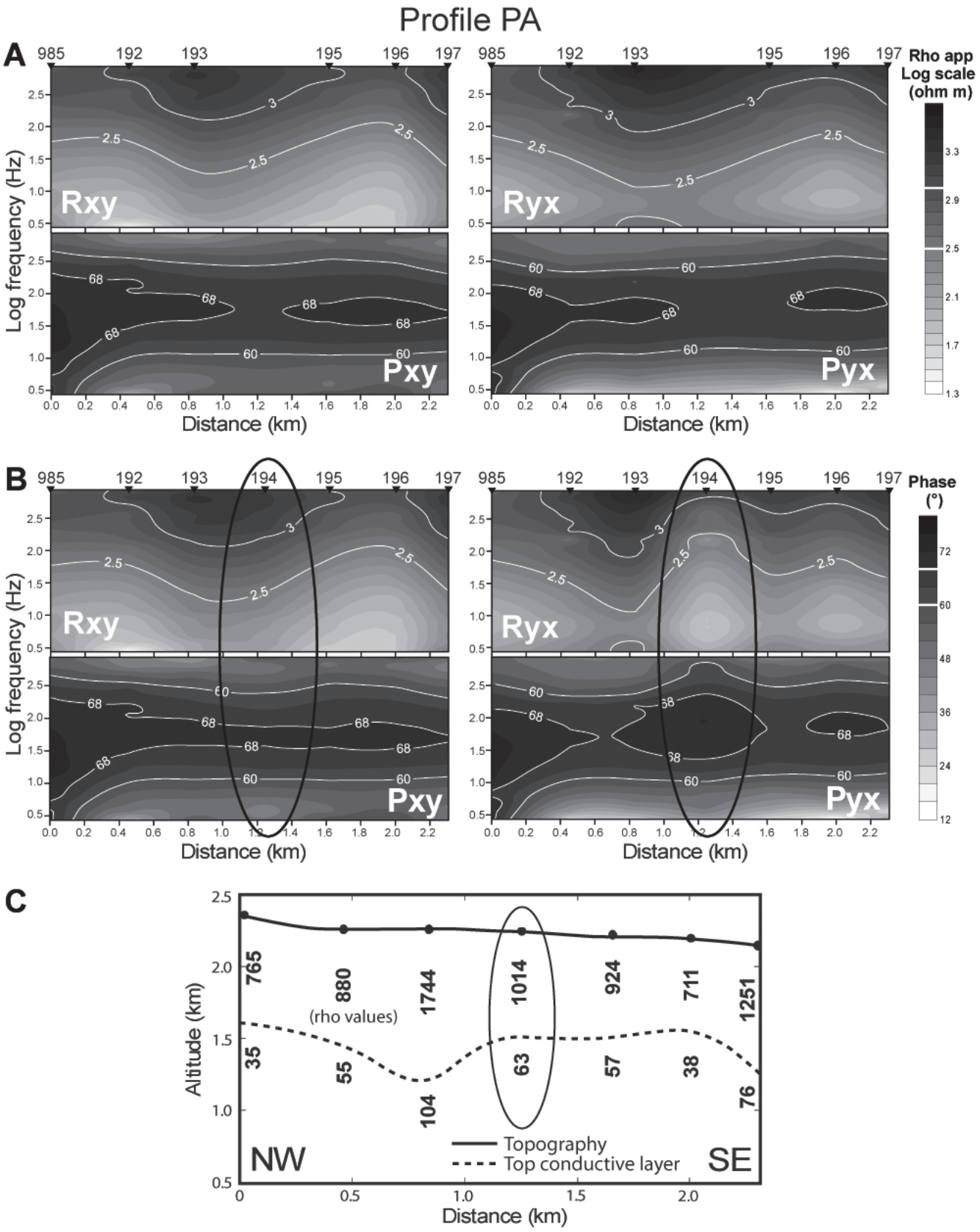

FIGURE 5 | **Example of a near 1-D behavior (profile PA Siete Fuentes - Fasnia area). A) Profile without site 194. Apparent resistivity and phase pseudosections for both polarizations. B) Profile with site 194 (surrounded by an ellipse). Apparent resistivity and phase pseudosections for both polarizations. C) True resistivity cross-section from 1-D modelling results. Black line is the topography. Dashed line is the top conductive layer.**

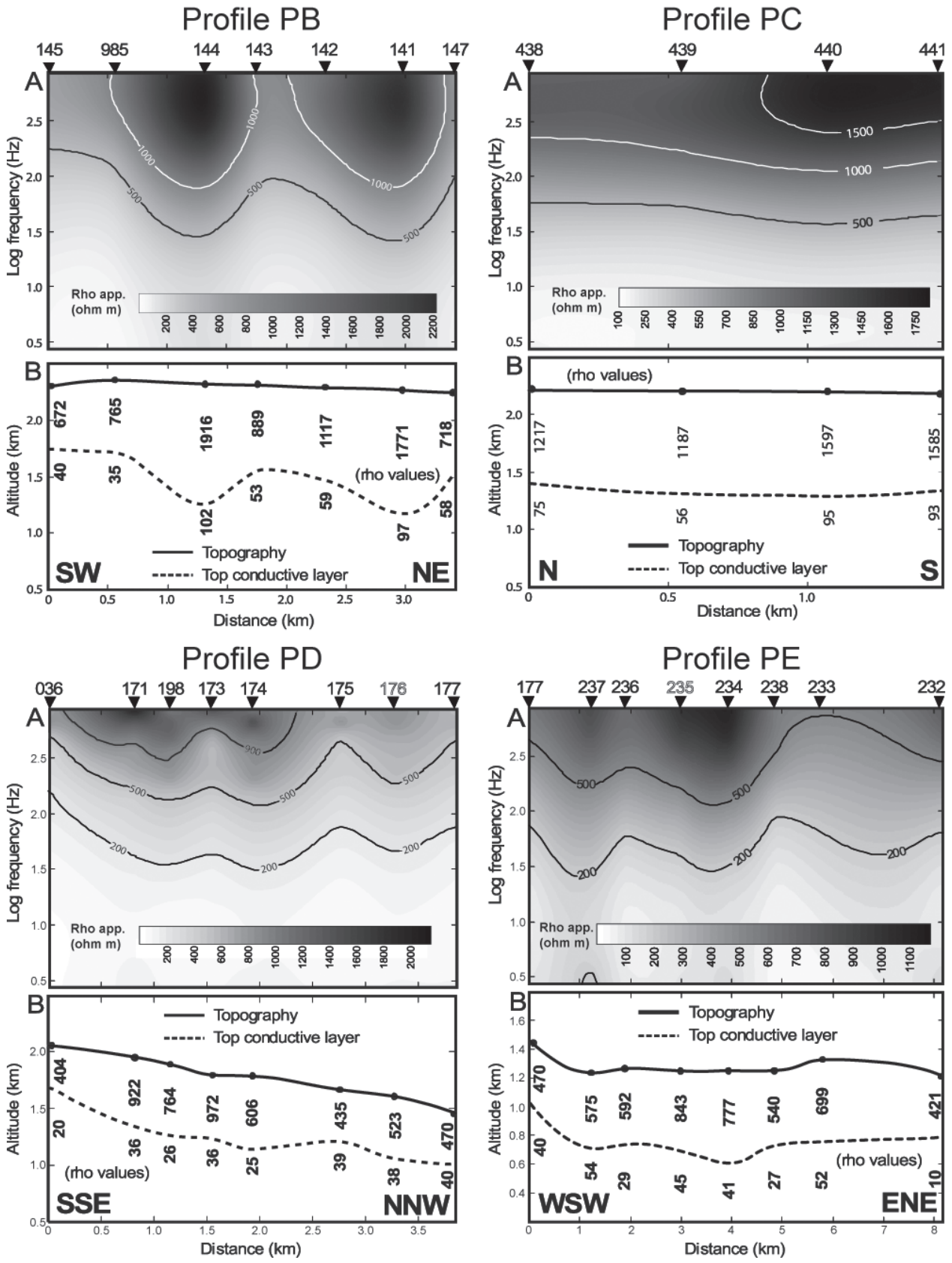

FIGURE 6 | **Profiles PB, PC, PD and PE (Siete Fuentes - Fasnia area and Orotava valley, Fig. 2). For each profile: A) Resistivity pseudosection based on the invariant of the impedance tensor. B) True resistivity cross-section from 1-D modelling results. Black line is the topography. Dashed line is the top conductive layer. The sites with enhanced names (top of pseudosections) are shown on Fig. 2.**

in the central part of Tenerife (Coppo et al., 2007b) show that conductive bodies are more developed along deeply rooted faults with implications not only on the volcanic edifice stability but also on groundwater flows. Around the Las Cañadas caldera, the origin of the conductive layer differs given its location. Two geological provinces must be considered: the flanks of the volcano and the upper part of it that includes calderas.

One conductive layer - two possible origins

The first geological province includes the flanks of Tenerife that have been deeply cut by flank collapse (Watts and Masson, 1995; Teide Group, 1997), i.e., the Orotava valley (profiles PD and PE, Fig. 2), the Guïmar valley (profile PF) and the Icod valley (Coppo et al., 2007a). The resistivity values of the conductive layer in these environments are characteristic. They are generally less than 60 Ωm, with very few exceptions. Geological data collected in the numerous galleries drilled for water supply reveal the presence of an impermeable plastic breccia within a clayish matrix that has been encountered both in the Orotava and the Icod valleys (Bravo, 1962; Coello, 1973; Navarro and Coello, 1989; Navarro Latorre, 1996). These authors interpreted this breccia either as the result of a flank collapse or as a "lubricating level" forming the base of the valleys. Because of its physical characteristics, this breccia has never been perforated, but its thickness is estimated to 300 m (Navarro Latorre, 1996). Similar thick layers formed during isolated events and generated by super faulting have been reported by Spray (1997). In our case, according to these field observations, we interpret the conductive layer highlighted at the base of the Orotava, Icod and Guïmar valleys as a breccia with a clayish matrix. Related to major collapse events, its common origin is a strong argument to explain the homogenous low resistivity observed. These results do not exclude the subsequent occurrence of hydrothermal alteration.

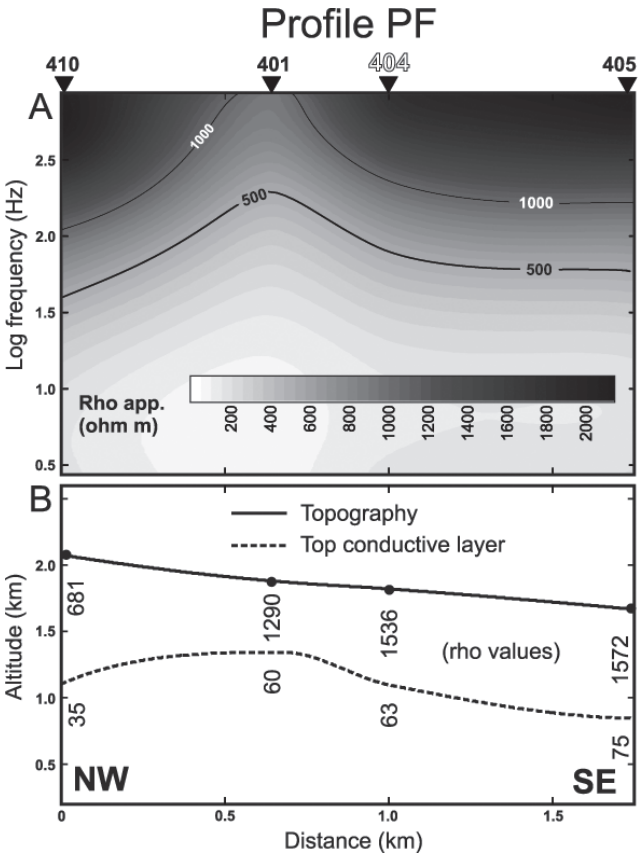

FIGURE 7 | **Profile PF (Guïmar valley, Fig. 2). A) Resistivity pseudosection based on the invariant of the impedance tensor. B) True resistivity cross-section from 1-D modelling results. Black line is the topography. Dashed line is the top conductive layer. The sites with enhanced names (top of pseudosection) are presented on Fig. 2.**

The second geological province characterizes the upper part of Tenerife, directly related to the main tectonic axis (rift zones) responsible for the growth of the NE-SW, NW-SE and SSW-NNE parts of the island (Galindo et al., 2005). As far as the subsurface of Tenerife is known, it includes the Las Cañadas caldera and its eastern part extending northeastwards on the Dorsal ridge (Fig. 1). In this part, there is no direct observation allowing a similar interpretation. However, the recent MT and AMT works interpreted the shallow conductive layer as a consequence of hydrothermal alteration (Pous et al., 2002; Coppo et al., 2007b). In the LCC, the authors interpreted the resistivity pattern of the conductive layer as a key to understanding caldera collapse processes and to locating ring faults. They noted that such structural features are characterized by massive conductive bodies generated by hydrothermal circulation along them (Coppo et al., 2007b). In a similar way, we interpret the conductive layer emphasized in the eastern LCC (profiles PA, PB and PC) as a result of hydrothermal circulations that generated alteration during volcanic activity along the Dorsal ridge. The layer affected by hydrothermal alteration corresponds approximately to the Old Basalts Series or to the "mortalón" (PNUD-UNESCO, 1973; Caloz, 1987). Benderitter et Gérard (1984) in La Réunion Island (F) observed that the relationship between the depth and the resistivity highlights the diffusive property of the hydrothermal alteration processes. Thus, the morphology of the top conductive layer reveals zones where intensity of these alteration processes was stronger and reached the upper surface. In that way, the hills characterizing the top conductive layer may reflect old volcanic fissures or fault zones.

What can be inferred from the morphology?

In the Orotava valley, the "wavy-like" structure of the top conductive layer suggests that this deep scar has

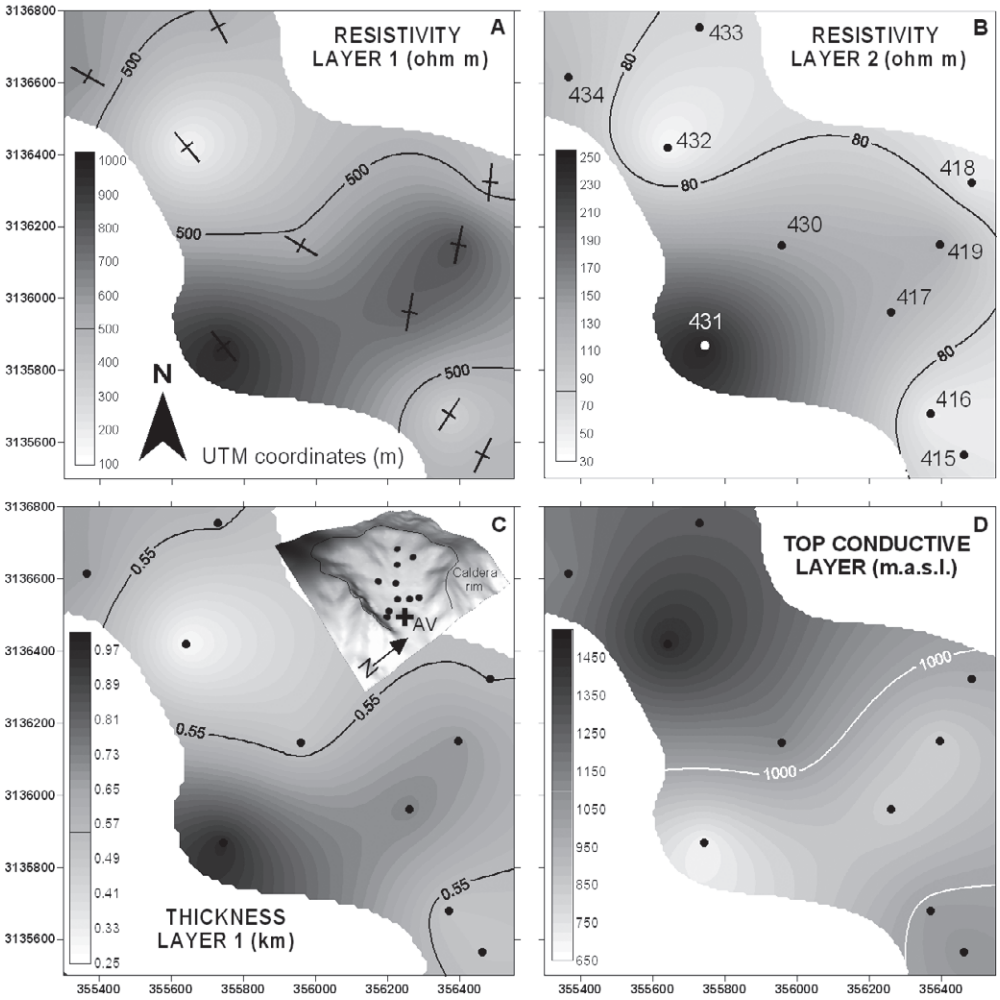

FIGURE 8 | **Interpolated results of 1-D modelling of the invariant of impedance tensors measured in the Pedro Gil caldera (PG area, Fig. 2). Inset in C: Shaded relief map of the Pedro Gil caldera with the rim emphasized by a black line and the Arafo volcano by a cross (AV). A) Resistivity of first resistive layer with isoline 500 Ωm. Short black lines indicate the strike direction from the phase anisotropy (mod 180°). B) Resistivity of the second conductive layer with isoline 80 Ωm and AMT sites. The site with enhanced name (top) is presented on Fig. 2. C) Thickness of the first resistive layer with isoline 0.55 km. D) Elevation of the top conductive layer with isoline 1000 m.a.s.l.**

been generated by separate landslides in agreement with Hürlimann et al. (2004). The western part extends to 4.5 km of profile PE (Figs. 6 & 9) and is slightly deeper than the eastern one. This "multiple landslides" hypothesis is strongly supported by off-shore observations (Watts and Masson, 1995). Moreover, the morphology of the top conductive layer in the Orotava valley allows computing a post-landslide infill of -55 km^3 of lavas (5 km^2 section and 11 km off-shore length). Considering the elevation of the lateral cliffs delimiting this huge scar, an on-shore volume higher than 100 km^3 has probably been removed by successive landslides.

Main structural features act as preferential paths for eruptions and also as headwalls of large lateral landslides. For instance, several authors extend the Orotava valley headwall up to the fracture responsible for historical eruptions (Figs. 9 & 10) (Marti et al., 1997; Hürlimann et al., 2004). Other authors constrain the location of the Teide - Pico Viejo Complex and the headwall of the Icod valley on the rift axis (Ablay and Marti, 2000). In order to constrain previous interpretations, we compared the morphology of the profiles PD (Orotava valley, Fig. 6), PF (Guïmar valley, Fig. 7) and a radial profile Teide – Pico Viejo Complex carried out in the Icod valley (Coppo et al., 2007a). In the three cases, the upper part of each profile shows the steepest dip with 34%, 65% and 36-60% for the Orotava, Guïmar and Icod valleys, respectively. These results indicate that headwalls of flank collapses are characterized by a steep ascent of the top conductive layer at shallow depth. Thus, an extrapolation of the top conductive layer toward the surface, would locate the headwall of the Orotava valley at around 700 m southwards from site 036, i.e., at the end of the LCC wall (Fig. 9 & 10). Eastwards however, its extension cannot be constrained accurately by the profile PB (Fig. 6). There, the headwall would be located slightly to the north at the end of the profile PB (Fig. 9) where the conductive layer depicts a steep ascent (site 147, Fig. 6). This implies that the upper part of the Orotava valley (Figs. 9 & 10), between the postulated position of the headwall and the total extension reaching the SW-NE fault (Marti et al., 1997; Hürlimann

et al., 2004), would constitute the "upper collapse of the Orotava valley".

In the Guïmar valley, the steep ascent of the conductive layer occurs between sites 401 and 404 (Fig. 7) around 1 km away from the current topographic headwall (the crest of the Dorsal ridge). Extending the fracture that links up Siete Fuentes to Arafo volcanoes, we find that the conductive feature of profile PF (Fig. 7) is located exactly above it (Fig. 9 & 10). Thus, we suggest that this conductive zone reveals the presence of this major fracture (Valentin et al., 1990) at depth and we interpret the fault plane as the headwall of the Guïmar landslide (Figs. 9 & 10). The space between the crest of the Dorsal ridge and the major fault reveals the volume eroded during the last 0.8 My and has major implications for the Pedro Gil caldera extension.

A major fault?

While profile PA (Fig. 5) displays a conductive feature exactly below the volcanic cones, no comparison can be made with the profile PC (Fig. 6), where the top conductive layer is flat. We interpret the conductive anomaly of profile PA as the activity of a hydrothermal system associated with the historic Siete-Fuentes fissural

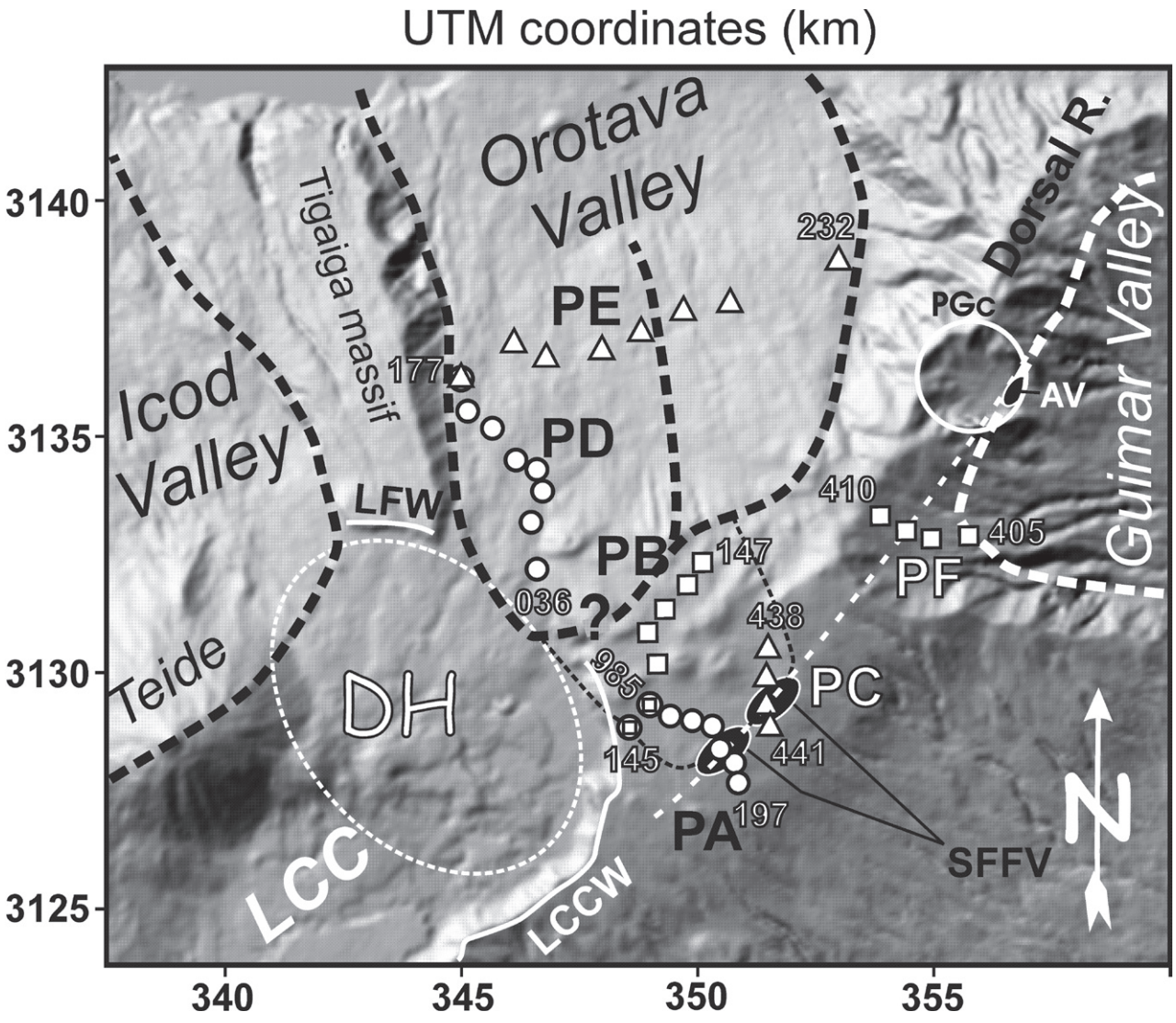

FIGURE 9 | **Extension of the lateral collapses. Thick black dashed lines show the extension Orotava valleys as inferred from the results (Icod from Coppo et al., 2007a). Thin black dashed line shows the uppermost part of the Orotava valley as inferred by Marti et al. (1997) and Hürlimann et al. (2004). Thick white dashed line shows the trace of the upper part of the Guïmar valley with a headwall constrained by the SW-NE fault (thin white dashed line). White circle indicates the Pedro Gil caldera (PGc). Small black ellipses are the historic eruptions (Siete Fuentes - Fasnia (SFFV) and Arafo volcanoes (AV)). AMT sites and profiles are similar to Fig. 2. LFW: La Fortaleza wall; LCCW: Las Cañadas caldera wall.**

eruption along the major SW-NE fault (Valentin et al., 1990). The lack of conductive anomaly on the profile PC (Fasnia volcano) suggests either the absence of hydrothermal circulation in this area or a deeper system. The first hypothesis is supported by higher concentrations of Rn close to the Siete Fuentes (western volcanoes, Fig. 2) (Hernández et al., 2003). Likewise, a temperature anomaly is measured closer to Siete Fuentes volcanoes than it is to Fasnia volcanoes (Valentin et al., 1990). Northeastwards, the fault reaches the aforementioned profile PF, and Arafo volcano, located on the rim of the Pedro Gil caldera (Fig. 10).

Is the Pedro Gil caldera tectonically controlled?

How can such a small caldera be located at the middle head of the Guïmar valley (Fig. 9)? A volcano collapse is responsible for the total destruction of the rocky environment, breaking volcanic structures and shaking the entire massif, resulting in a huge central chaotic breccia (Lipman, 1999). This event generates permeable connections and preferential pathways between deeper parts of the volcanic edifice and the surface. These pathways ease migration of heat, gas and fluids towards the surface and allow strong hydrothermal alteration of rocks (Pous et al., 2002; Hernández et al.,

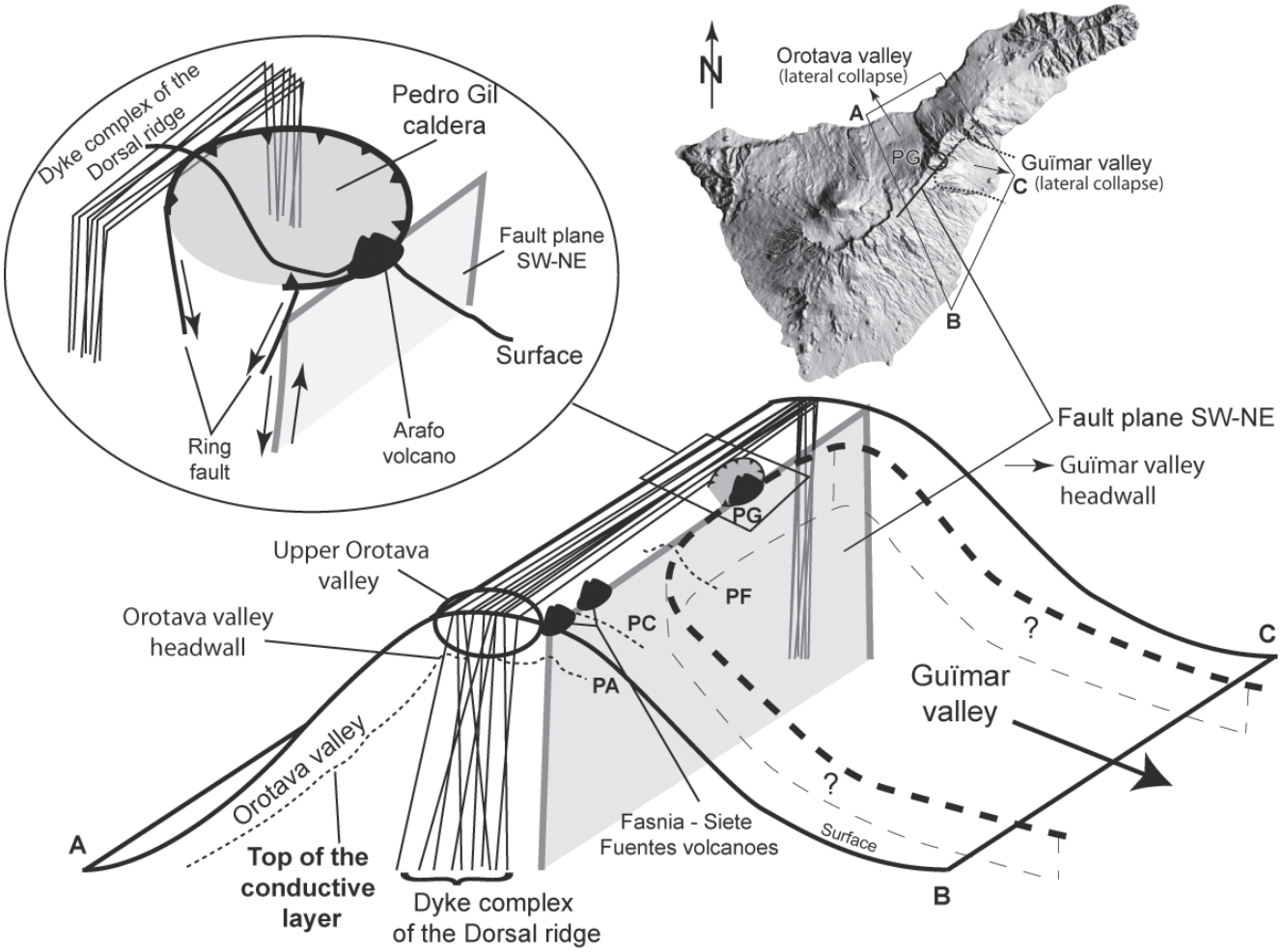

FIGURE 10 | **Simplified structural sketch of the eastern part of the Las Cañadas caldera. Upper right corner: Shaded relief map of Tenerife showing the 3D bloc illustrated below (with A, B, C corners). Black dashed line: trace of the Guïmar landslide. Black line: SW-NE fault connecting historical eruptions. Small white circle: Pedro Gil caldera. 3D bloc showing: SW-NE fault plane (transparent light grey); the three volcanoes related to historical eruptions; 3 schematized profiles PA, PC and PF; the dike complex of the Dorsal ridge; the Guïmar landslide in a pseudo 3D view (question marks indicate the absence of data in the medium and lower parts); top of the conductive layer is shown by a thin dashed line; Orotava valley headwall corresponds to the upper limit of the valley as shown in Fig. 9 (thick dashed line); the upper Orotava valley indicates the zone between the two proposed extensions (see text and Fig. 2). Upper left: zoom enlargement of the Pedro Gil caldera showing its incomplete ring fault open to the SW and its extension between the dike complex of the Dorsal ridge and the major fault plane.**

2003; Galindo et al., 2005). Finally, these processes lead to the formation of a thick, mainly clayey conductive layer. This layer could be interpreted as a clay horizon belonging to an ancient phase of the volcano which acts as a temporal marker (Schnegg, 1997).

We interpret the morphology of the top conductive layer (Fig. 8D), as for the LCC (Coppo et al., 2007b), in terms of caldera forming processes. Thus, it constitutes a possible morphology consecutive to the volcano collapse, in which the higher and more conductive areas delimit the original caldera (Coppo et al., 2007b). It is characterized by an elongated, NE-axed depression, with almost 800 m between the lower and higher parts. The width of the caldera between sites 432 and 415 is about 1300 m. Northeastwards, the conductive layer forms a semicircular zone of lower resistivity (< 80 m), that allows drawing half a ring fault, more or less parallel to the 80 m isoline (Fig. 8B).

For the formation of the Pedro Gil caldera, the lack of conductive rocks in the SW part suggests a trapdoor subsidence rather than a piston model. Bounded by a partial ring fault and a hinged segment, the trapdoor subsidence constitutes an incomplete or incipient plate collapse, a process mid way between plate and down sag subsidence. Such partial subsidence may be related to smaller eruptions, an asymmetric magma chamber or some regional structural influences (Varga and Smith, 1984; Lipman, 1999). The structure is clearly revealed by the maximum phase anisotropy of the ten AMT soundings, as well as coherent strikes related either to the Dorsal ridge or to the NE-SW major fault (Fig. 8A).

Figure 10 diagrammatically resumes the structural setting between the eastern part of the LCC and the Pedro Gil caldera. At the end of a period of strong volcanic activity, the Pedro Gil edifice collapsed after the breaking of the magma chamber roof (Galindo, 2005). Because of the local structural setting, the collapse has been controlled and limited by both the SW-NE fault (SE) and the dike complex of the Dorsal ridge (NW), between which, the magma chamber developed. This structural sketch strongly supports the idea that the Pedro Gil caldera collapse initiated the Guïmar landslide (0.81 My, Ancochea et al., 1990), a hypothesis recently proposed by Galindo (2005).

CONCLUSIONS

This paper presents the morphology of a widespread, shallow conductive layer that has been identified in four characteristic geological provinces (Orotava valley, Siete Fuentes - Fasnia zone, Guïmar valley and Pedro Gil caldera) of the eastern part of the Las Cañadas caldera (Canary Islands), using fifty AMT tensors. Results argue that the conductive layer is a consequence of two different processes: a) according to geological data, the conductive layer characteristic of the flanks is interpreted as a plastic breccia with a clayish matrix generated during huge lateral collapse; and b) along main tectonic structures and inside calderas, it is formed by hydrothermal alteration processes. In both areas, the results suggest that the conductive layer is related to major structural volcanic events (flank collapse or caldera collapse) and can be seen as a temporal marker of the island evolution.

The slope of the top conductive layer in the upper part of the valley suggests headwall locations of the giant landslides that affected the flanks of Tenerife. The Orotava headwall would be located close to the eastern end of the Las Cañadas caldera wall. Its uppermost part has probably been affected by secondary processes related to dike intrusion or fissure eruptions along the Dorsal ridge. The AMT profiles carried out between Siete-Fuentes and Arafo volcanoes strongly support that the headwall of the Guïmar valley is parallel to a SW-NE major fault, a preferential path of structural weakness responsible for three historic eruptions.

Investigations in the Pedro Gil caldera confirm that the initial caldera was smaller than it currently is. Furthermore, the absence of conductive rocks in its SW part suggests that the caldera does not result from vertical collapse but rather from trapdoor subsidence. The major SW-NE fault that connects historic eruptions and the NE rift axis (Dorsal ridge) controlled the extension of the Pedro Gil caldera collapse. These data support the origin of the Guïmar lateral collapse as mechanically initiated by the Pedro Gil caldera collapse.

In summation, these results demonstrate that shallow conductive layers contain some crucial keys to improving the knowledge of the structural evolution of volcanic edifices.

ACKNOWLEDGMENTS

This project has been financed through grants from the Swiss National Science Foundation (SNSF, project N°200020-111758). We gratefully acknowledge the help of Dr. Joan Martí (CSIC Barcelona) for field facilities. Critical and constructive reviews by Dr. Adele Manzella and Dr. Yasuo Ogawa strongly improved the manuscript.

REFERENCES

Abdel-Monem, A.N., Watkins, N., Gast, P., 1972. Potassium-argon ages, volcanic stratigraphy and geomagnetic polarity

history of the Canary Islands: Tenerife, La Palma and Hierro. American Journal of Sciences, 272, 805-825.

Ablay, G.J., Marti, J., 2000. Stratigraphy, structure, and volcanic evolution of the Pico Teide-Pico Viejo formation, Tenerife, Canary Islands. Journal of Volcanology and Geothermal Research, 103, 175-208.

Aizawa, K., Yoshimura, R., Oshiman, N., Yamazaki, K., Uto, T., Ogawa, Y., Tank, S.B., Kanda, W., Sakanaka, S., Furukawa, Y., Hashimoto, T., Uyeshima, M., Ogawa, T., Shiozaki, I., Hurst, A.W., 2005. Hydrothermal system beneath Mt. Fuji volcano inferred from magnetotellurics and electric self-potential. Earth and Planetary Science Letters, 235, 343-355.

Ancochea, E., Huertas, M.J., Cantagrel, J.M., Coello, J., Fúster, J.M., Arnaud, N., Ibarrola, E., 1999. Evolution of the Cañadas edifice and its implications for the origin of the Cañadas Caldera (Tenerife, Canary Islands). Journal of Volcanology and Geothermal Research, 88, 177-199.

Ancochea, E., Fúster, J.M., Ibarrola, E., Cendrero, A., Coello, J., Hernán, F., Cantagrel, J.M., Jamond, C., 1990. Volcanic evolution of the island of Tenerife (Canary Islands) in the light of new K-Ar data. Journal of Volcanology and Geothermal Research, 44, 231-249.

Araña, V., 1971. Litologia y estructura del Edificio Cañadas, Tenerife (Islas Canarias). Estudios Geologicos, XXVII, 95-135.

Ballestracci, R., Nishida, Y., 1987. Fracturing associated with the 1977-1978 eruption of Usu volcano, north Japan, as revealed by geophysical measurements. Journal of Volcanology and Geothermal Research, 34, 107-121.

Benderitter, Y., Gérard, A., 1984. Geothermal study of Reunion island: audiomagnetotelluric survey. Journal of Volcanology and Geothermal Research, 20, 311-332.

Boubekraoui, S., Courteaud, M., Aubert, M.A., Y., Coudray, J., 1998. New insights into the hydrogeology of a basaltic shield volcano from comparison between self-potential and electromagnetic data: Piton de la Fournaise, Indian Ocean. Journal of Applied Geophysics, 40, 165-177.

Bravo, T., 1962. El Circo de Las Cañadas y sus dependencias. Boletín Real Sociedad Española de Historia Natural, 40, 93-108.

Cagniard, L., 1953. Basic theory of the magnetotelluric method of geophysical prospecting. Geophysics, 18(3), 605-635.

Caloz, P., 1987. Galeries de captage d'eau sur l'île de Tenerife. Iles Canaries, Espagne. Etude des courbes de tarissements. Diploma Thesis. University of Neuchâtel, Switzerland, 67 pp.

Coello, J., 1973. Las series volcánicas de los subsuelos de Tenerife. Estudios Geológicos, 29(6), 491-512.

Coppo, N., Schnegg, P.-A., Falco, P., Costa, R., 2009. A deep scar in the flank of Tenerife (Canary Islands): Geophysical contribution to tsunami hazard assessment. Accepted for publication in Earth Planetary Science Letters. Doi:10.1016/j.epsl.2009.03.017

Coppo, N., Schnegg, P.-A., Falco, P., Heise, W., Costa, R., 2007b. Multiple caldera collapses inferred from the shallow electrical resistivity signature of the Las Cañadas caldera, Tenerife, Canary Islands. Journal of Volcanology and Geothermal Research, 170(3-4), 153-166.

Courteaud, M., Ritz, M., Robineau, B., Join, J.-L., Coudray, J., 1997. New geological and hydrogeological implications of the resistivity distribution inferred from audiomagnetotellurics over La Fournaise young shield volcano (Reunion Island). Journal of Hydrology, 203, 93-100.

Descloitres, M., Ritz, M., Robineau, B., Courteaud, M., 1997. Electrical structure beneath the eastern collapsed flan of Piton de la Fournaise volcano, Reunion Island: Implications for the quest for groundwater. Water Resources Research, 33 (1), 13-19.

Filloux, J., 1987. Instrumentation and experimental methods for oceanic studies. In: Jacobs (ed.). Geomagnetism. London, Academic Press, vol. 1 (3rd edition), 143-248.

Fischer, G., Le Quang, B.V., 1981. Topography and minimization of standard deviation in one-dimensional magnetotelluric inversion scheme. Geophysical Journal Royal Astronomical Society, 67, 279-292.

Fuji-ta, K., Ogawa, Y., Ichiki, M., Yamaguchi, S., Makino, Y., 1999. Audio frequency magneto-telluric (AMT) survey of Norikura Volcano in central Japan. Journal of Volcanology and Geothermal Research, 90, 209-217.

Fúster, J.M., Araña, V., Brandle, J.L., Navarro, M., Alonso, U., Aparicio, A., 1968. Geología y vulcanología de las Islas Canarias, Tenerife. Madrid, Special publication Instituto Lucas Mallada del CSIC, 218 pp.

Galindo, I., 2005. Estructura volcano-tectónica y emisión difusa de gases de Tenerife (Islas Canarias). Doctoral Thesis. Barcelona (Spain), Universidad de Barcelona, 398 pp.

Galindo, I., Soriano, C., Martí, J., Pérez, N., 2005. Graben structure in the Las Cañadas edifice (Tenerife, Canary Islands): implications for active degassing and insights on the caldera formation. Journal of Volcanology and Geothermal Research, 144(1-4), 73-87.

Hernández, P., Pérez, N., Salazar, J., Reimer, M., Notsu, K., Wakita, H., 2003. Radon and helium in soil gases at Cañadas caldera, Tenerife, Canary Islands, Spain. Journal of Volcanology and Geothermal Research, 2721, 1-18.

Hürlimann, M., Marti, J., Ledesma, A., 2004. Morphological and geological aspects related to large slope failures on oceanic islands. The huge La Orotava landslide on Tenerife, Canary Islands. Geomorphology, 62(3-4), 143-158.

Ibarrola, E., Ancochea, E., Fúster, J.M., Cantagrel, J.M., Coello, J., Snelling, N.J., Huertas, M.J., 1993. Cronoestratigrafia del Macizo de Tigaiga: Evolución de un sector del edificio Cañadas (Tenerife, Islas Canarias). Boletín Real Sociedad Española de Historia Natural, 88(1-4), 57-72.

Krastel, S., Schmincke, H.-U., Jacobs, C.L., Rihm, R., Le Bas, T.P., Alibès, B., 2001. Submarine landslides around the Canary Islands. Journal of Geophysical Research, 106, 3977-3997.

Lipman, P.W., 2000. Caldera. In: Sigurdsson, H., Houghton, B.F., McNutt, S.R., Rymer, H., Stix, J. (eds.). Encyclopedia of Volcanoes. San Diego, Academic Press, 643-662.

Manzella, A., Volpi, G., Zaja, A., Meju, M., 2004. Combined TEM-MT investigation of shallow-depth resistivity structure of Mt Somma-Vesuvius. Journal of Volcanology and Geothermal Research, 131, 19-32.

Marti, J., 1998. Comment on "A giant landslide on the northern flank of Tenerife, Canary Island" by A. B. Watts and D.G. Masson. Journal of Geophysical Research, 103(B5), 9945-9947.

Marti, J., Gudmundsson, A., 2000. The Las Cañadas caldera (Tenerife, Canary Islands): an overlapping collapse caldera generated by magma-chamber migration. Journal of Volcanology and Geothermal Research, 103, 161-173.

Marti, J., Mitjavila, J., Araña, V., 1994. Stratigraphy, structure and geochronology of the Las Cañadas Caldera (Tenerife, Canary Islands). Geological Magazine, 131 (6), 715-727.

Marti, J., Hürlimann, M., Ablay, G.J., Gudmundsson, A., 1997. Vertical and lateral collapses on Tenerife (Canary Islands) and other volcanic oceanic islands. Geology, 25, 879-882.

Masson, D.G., Watts, A.B., Gee, M.J.R., Urgeles, R., Mitchell, N.C., Le Bas, T.P., Canales, M., 2002. Slope failures on the flanks of the western Canary Islands. Earth-Science Reviews, 57, 1-35.

Matsushima, N., Oshima, H., Ogawa, Y., Takakura, S., Satoh, H., Utsugi, M., Nishida, Y., 2001. Magma prospecting in Usu volcano, Hokkaido, Japan, using magnetotelluric soundings. Journal of Volcanology and Geothermal Research, 109, 263-277.

Monteiro Santos, F.A., Trota, A., Soares, A., Luzio, R., Lourenço, N., Matos, L., Almeida, E., Gaspar, J.L., Miranda, J.M., 2006. An audio-magnetotelluric investigation in Terceira Island (Azores). Journal of Applied Geophysics, 59(4), 314-323.

Müller, A., Haak, V., 2004. 3-D modeling of the deep electrical conductivity of Merapi volcano (Central Java): integrating magnetotellurics, induction vectors and the effects of steep topography. Journal of Volcanology and Geothermal Research, 138, 205-222.

Navarro, J.M., Coello, J., 1989. Depressions originated by landslide processes in Tenerife. In: Araña, V. (ed.). Lanzarote, European Science Foundation Meeting on Canarian Volcanism, 150-152.

Navarro Latorre, J.M., 1996. Hydrogeological analysis of the Las Cañadas area (in Spanish). In: Excelentísimo Cabildo Insular. Estudios hidrogeológicos de Tenerife. Tenerife, Excelentísimo Cabildo Insular, 1-64.

Nurhasan, Ogawa, Y., Ujihara, N., Tank, B., Honkura, Y., Onizawa, S., Mori, T., Makino, M., 2006. Two electrical conductors beneath Kusatsu-Shirane volcano, Japan, imaged by audiomagnetotellurics, and their implications for the hydrothermal system. Earth Planets Space, 58, 1053-1059.

Ogawa, Y., Takakura, S., 1990. CSAMT Measurements across the 1986 C Craters of Izu-Oshima Island, Japan. Journal of Geomagnetism and Geoelectricity, 42, 211-224.

Ogawa, Y., Matsushima, N., Oshima, H., Takakura, S., Utsugi, M., Hirano, K., Igarashi, M., Doi, T., 1998. A resistivity cross-section of Usu volcano, Hokkaido, Japan, by audiomagnetotelluric soundings. Earth Planets Space, 50, 339-346.

Ortiz, R., Araña, V., Astiz, M., García, A., 1986. Magnetotelluric study of the Teide (Tenerife) and Timanfaya (Lanzarote) volcanic areas. Journal of Volcanology and Geothermal Research, 30(3-4), 357-377.

MOP-UNESCO, 1975. Estudio científico de los recursos de agua en las Islas Canarias (SPA/69/515). Madrid, Ministerio de Obras Públicas, Dirección General de Obras Hidráulicas, Programa de las Naciones Unidas para el Desarrollo (UNESCO). Volúmenes III (238pp) and V (illustrations).

Pous, J., Heise, W., Schnegg, P.-A., Muñoz, G., Marti, J., Soriano, C., 2002. Magnetotelluric study of the Las Cañadas caldera (Tenerife, Canary Islands): structural and hydrogeological implications. Earth and Planetary Science Letters, 204, 249-263.

Schnegg, P.-A., 1993. An automatic scheme for 2-D magnetotelluric modelling, based on low-order polynomial fitting. Journal of Geomagnetism and Geoelectricity, 45, 1039-1043.

Schnegg, P.-A., 1997. Electrical structure of Plaine des Sables caldera, Piton de la Fournaise volcano (Reunion Island). Annali di Geofisica, XL(2), 305-317.

Servicio de Planificación Hidráulica, 1993. Plan hidrológico insular de Tenerife. Tenerife, Gobierno de Canarias, 138pp.

Simpson, F., Bahr, K., 2005. Practical Magnetotellurics. Cambridge, Cambridge University Press, 254 pp.

Spray, J.G., 1997. Superfaults. Geology, 25(7), 579-582.

Teide Group, 1997. Morphometric interpretation of the northwest and southeast slopes of Tenerife, Canary Islands. Journal of Geophysical Research, 102(B9), 20325-20342.

Valentin, A., Albert-Beltran, J.F., Diez, J.L., 1990. Geochemical and geothermal constraints in magma bodies associated with historic activity, Tenerife (Canary Islands). Journal of Volcanology and Geothermal Research, 44, 251-264.

Varga, R.J., Smith, B.M., 1984. Evolution of the early Oligocene Bonanza caldera, northeast San Juan volcanic field, Colorado. Journal of Geophysical Research, 89, 8679-8694.

Vozoff, K., 1991. The magnetotelluric method. In: Nabighian, M.N. (ed.). Electromagnetic Methods in Geophysics. Oklahoma (USA), Society of Exploration Geophysicists Tulsa, 641-711.

Watts, A.B., Masson, D.G., 1995. A giant landslide on the north flank of Tenerife, Canary Islands. Journal of Geophysical Research, 100(B12), 24487-24498.